NASA TN D-534

TECHNICAL NOTE

D-534

HOVERING MEASUREMENTS FOR TWIN-ROTOR CONFIGURATIONS

WITH AND WITHOUT OVERLAP

By George E. Sweet

Langley Research Center
Langley Field, Va.

NATIONAL AERONAUTICS AND SPACE ADMINISTRATION

WASHINGTON

November 1960

NATIONAL AERONAUTICS AND SPACE ADMINISTRATION

TECHNICAL NOTE D-534

HOVERING MEASUREMENTS FOR TWIN-ROTOR CONFIGURATIONS WITH AND WITHOUT OVERLAP

By George E. Sweet

SUMMARY

Results of an investigation in the Langley full-scale tunnel of the hovering performance of large-scale twin-rotor-helicopter models are presented. Measurements of thrust, torque, and rotor flapping are given for overlapped (approximately 76 percent of blade radius) and nonoverlapped configurations and for two different rotor solidities. The measured performance is compared with single-rotor measurements and with available rotor theory. These tests show that the hovering performance of a single rotor and of two rotors without overlap or vertical offset are the same and hence may be calculated by single-rotor theory. These tests in conjunction with results of previous coaxial-rotor tests show that the performance of highly overlapped rotors can be reasonably predicted by available rotor theory.

INTRODUCTION

The hovering performance of a helicopter with more than one rotor may be greatly influenced by the mutual interference between rotors. Until recently there has been some question as to the accuracy of test results from twin-rotor helicopters, either because of scale effects or because of insufficiently accurate instrumentation. For example, the results of the twin-rotor tests of reference 1 indicate a large increase in hovering performance, whereas the data of reference 2, for essentially the same configuration, show no increase in performance.

In order to study the effects of mutual interference between rotors, tests of a large twin-rotor-helicopter model have been conducted in the Langley full-scale tunnel. The model was constructed to allow changes in the rotor spacing; thus permitting examination of the effect of rotor overlap on performance. The present instrumentation is greatly improved over that used in the tests of reference 1, inasmuch as the performance of each rotor was measured individually.

The data (portions of which were presented previously in ref. 3) are compared with available theory in order to indicate the degree to which the performance of rotor systems with various degrees of overlap may be predicted.

SYMBOLS

a slope of curve of section lift coefficient against section angle of attack in radians

b number of blades per rotor

a_1 coefficient of $-\cos\psi$ in expression for β; hence, longitudinal tilt of rotor cone with respect to axis of no feathering, positive for rearward tilt

b_1 coefficient of $-\sin\psi$ in expression for β; hence, lateral tilt of rotor cone with respect to axis of no feathering, positive for tilt toward advancing side

C_T rotor-thrust coefficient, $\dfrac{T}{\pi R^2 \rho (\Omega R)^2}$

C_Q rotor-torque coefficient, $\dfrac{Q}{\pi R^2 \rho (\Omega R)^2 R}$

c blade section chord, ft

c_e equivalent blade chord (on thrust basis), $\dfrac{\int_{r_c}^{R} cr^2 dr}{\int_{r_c}^{R} r^2 dr}$, ft

$c_{d,o}$ profile-drag coefficient of rotor-blade section

L distance between rotor shafts, ft

Q rotor torque, ft-lb

R blade radius, ft

r radial distance to blade element, ft

r_c radius of blade cutout, ft

T rotor thrust, lb

v induced inflow velocity at rotor (always positive), ft/sec

Z height of rotor above ground, ft

α_r blade-element angle of attack, measured from line of zero lift, $\theta - \phi$, radians

β blade-flapping angle at particular azimuth position, ($\beta = -a_1 \cos \psi - b_1 \sin \psi \ . \ . \ .$)

$\delta_0, \delta_1, \delta_2$ coefficients in power series expressing $c_{d,o}$ as function of α_r, $c_{d,o} = \delta_0 + \delta_1 \alpha_r + \delta_2 \alpha_r^2$

θ blade pitch angle, radians

λ inflow ratio $- \frac{v}{\Omega R}$ for hovering

ρ mass density of air, slugs/cu ft

σ rotor solidity, $bc_e/\pi R$

ϕ inflow angle in plane perpendicular to blade-span axis $\frac{v}{\Omega R}$, radians

ψ blade-azimuth angle measured from rearmost point of motor (see fig. 1(b)) in direction of rotation, radians

Ω rotor rotational velocity, radians/sec

Subscript:

t tip

APPARATUS AND TESTS

The tests were conducted in the Langley full-scale tunnel which is fully described in reference 4.

The helicopter model used in the present investigation is shown in figure 1. The rotors of this model may be spaced for operation with no

overlap or for a 76-percent-radius overlap (i.e., the ratio of radial overlap to blade radius). However, this overlap in terms of overlapped area is only 13 percent of the total disk areas. Because of the ambiguity of common methods of expressing overlap in percent, L/R (i.e., the ratio of shaft spacing to rotor radius) is used in this paper.

The rotor blades mounted on teetering hubs were phased 90° apart in azimuth and were located as shown in figure 1(b). All blades were untwisted, rectangular in planform, and had NACA 0012 airfoil sections. Blade planforms and dimensions are given in figure 1(c).

Two pairs of rotors having solidities of 0.0543 and 0.0968 were used in the current tests. The low-solidity rotors were 15 feet in diameter and the high-solidity rotors were 15.25 feet in diameter.

A large ground-reflection plane was located 15.6 feet below the rotors. The primary purpose of this plane was to minimize wind-tunnel jet-boundary corrections in the subsequent forward-flight tests. Since the rotors were located slightly over one-rotor diameter above the reflection plane, ground effect should be negligible for a single rotor. As pointed out in reference 3, ground effect should also be negligible for the twin-rotor configuration.

The thrust and torque of each rotor was measured independently using strain-gage instrumentation located in each rotor support (fig. 2). Thrust was electrically corrected for lifting loads imposed on the balance by blade-pitching moments. The frictional torque of the rotor-control mechanism was electrically subtracted from rotor-torque measurements. Blade-flapping and blade-feathering motions were sensed by strain gages and recorded on an oscillograph. A Fourier analysis was performed on these data to determine flapping and feathering coefficients. Rotor-rotational speed was measured with a sensitive aircraft tachometer. The overall accuracies of the data are believed to be as follows:

Thrust	±9 lb (2 percent)
Torque	±4 ft-lb (1 percent)
Rotor tip speed	±1 fps (0.2 percent)
Flapping and feathering motions	±0.25 deg

Although the absolute magnitude of blade motions are within ±0.25°, the repeatability of these data is within ±0.10°.

All tests were conducted at a tip speed of approximately 500 fps, which corresponds to a tip Reynolds number of 2.0×10^6 for the low-solidity rotors and 3.7×10^6 for the high-solidity rotors. Thrust, torque, flapping, and feathering motions were measured for several blade pitch angles for each configuration. Similar measurements were

made for each rotor with the other rotor removed; thus simulating a single-rotor configuration. The rotors were always trimmed for zero flapping with respect to the shaft; thus both rotors were maintained in the same plane.

RESULTS AND DISCUSSION

A comparison of measured rotor performance with theoretical calculations will be presented for the hovering case in plots of C_T against C_Q. In addition, the presence of rotor interference will be examined by comparing the measured flapping coefficients for each configuration.

Single Rotor

The performance of just one of the rotors, which will be used subsequently as a standard for comparison, is shown in figures 3 and 4. The calculated performance (see, for example, ref. 5) agrees almost perfectly with the single-rotor measurements. (The profile drag was assumed to be $c_{d,o} = \delta_0 + \delta_1 \alpha_r + \delta_2 \alpha_r^2$, where δ_0 was calculated from measured torque at zero lift and δ_1 and δ_2 were obtained from reference 6. A lift-curve slope $a = 5.55$, a function of Reynolds number, was determined by the method of reference 7. The tip-loss factor B was taken herein as

$$B = 1 - \frac{1.386}{b} \phi_t$$

rather than expressing it in terms of C_T, which requires an iterative integration. This form was obtained from the appendix of reference 8 by noting that $\lambda = \frac{v_t}{\Omega R} = \phi_t$ and that $\sqrt{1 + \lambda^2}$ is essentially equal to one.

Two Rotors Without Overlap

Figures 3 and 4 show that the performance of two nonoverlapped rotors is the same as that of two isolated rotors. Note that the tests of reference 1 had indicated a gain in rotor efficiency, because of mutual rotor interference, for this configuration. The present test results, however, using greatly improved instrumentation, indicate that gains in rotor efficiency for rotors without overlap are nonexistent.

As might be expected some minor interference effects do exist. Notice the presence of small amounts of equivalent rotor flapping (figs. 5 and 6).

The flapping measurements indicate that the inflow distribution is slightly altered; however, there must be no appreciable change of net inflow inasmuch as the performance is unaltered (figs. 3 and 4).

Two Rotors With Overlap

Figure 7 shows that when the test rotors were overlapped, the thrust of each rotor remaining unchanged, a substantial power increase resulted. Such a result would be expected since the local disk loading is greatly increased in the overlapped portion of the rotor disks. The increase in induced power for this configuration is approximately 14 percent (about an 11-percent increase in total power at $C_T = 0.0056$). Notice the large effect of mutual rotor interference on rotor flapping for the overlapped rotors (L/R = 1.23) as compared to the nonoverlapped rotors (L/R = 2.03) (fig. 8(a)). This would be expected as the loss of lift in the overlap region, resulting from greater inflow velocities, must be compensated for by increased flapping. Consequently, increases in rotor overlap, while maintaining the thrust of each rotor constant, result in increased induced-power requirements; the limit, of course, being for a coaxial arrangement where each rotor requires 41.4 percent more induced power than a single isolated rotor, in accordance with the increased disk loading (ref. 3).

Calculated Performance of Overlapped Rotors

The performance of the overlapped rotor configurations has been calculated by the methods of references 2 and 3, and is compared with the measured performance of the overlapped rotors in figure 9. For comparison, the calculated performance of an isolated single rotor is also given in figure 9.

The method of reference 2 uses momentum theory to obtain an induced velocity caused by the sum of the lift carried by rotors at any location in the overlapped region. This induced velocity was used in the usual blade-element equations in order to obtain rotor thrust and torque. The procedure of this paper differs slightly from that of reference 2 which uses momentum theory to obtain thrust; however, the results are essentially unaltered by the procedure chosen. In the course of the calculations, it was found that inclusion of blade-flapping terms did not alter the final result; therefore, it is permissible to neglect the flapping.

In the absence of ground effect $Z/R = \infty$, the method of reference 3 reduces to simple momentum theory. The performance of the overlapped rotors is obtained by merely multiplying the induced power of a single isolated rotor by the appropriate factor from the charts of reference 3.

Examination of figure 9 indicates that either method (ref. 2 or ref. 3) yields approximately the correct effect on performance of rotor overlap. Since this is the case, the use of reference 3 is indicated if for no other reason than its simplicity and ease of application.

Effect of Wake Blockage

In order to provide some insight into the effect of wake blockage, the present data are compared with unpublished results of a previous investigation of the same rotors in a tandem configuration. Notice that the fuselage size is greatly reduced for the tandem configuration (figs. 10(a) and 10(b)). Figures 11 and 12 show that the performance of the two configurations is in good agreement. Hence the effect of wake blockage, if any, is within the accuracy of measurement.

CONCLUSIONS

An investigation, in hovering, of a model with two lifting rotors, indicates that:

1. The performance of each rotor of a twin-rotor configuration having neither overlap nor vertical offset is essentially identical to that of a single isolated rotor. Consequently, the performance of the twin rotors can be calculated as if they were two single rotors.

2. For the test configuration with approximately 76-percent-radius overlap, 14 percent more induced power was required than for the two isolated rotors at the same total thrust. This increase was closely predicted by available rotor theory. The present tests and earlier coaxial rotor tests show that the hovering performance of highly overlapped rotors can be calculated with reasonable accuracy using available theory.

Langley Research Center,
National Aeronautics and Space Administration,
Langley Field, Va., July 28, 1960.

REFERENCES

1. Dingeldein, Richard C.: Wind-Tunnel Studies of the Performance of Multirotor Configurations. NACA TN 3236, 1954.

2. Stepniewski, W. Z.: A Simplified Approach to the Aerodynamic Rotor Interference of Tandem Helicopters. Proc. Second Annual Western Forum, Am. Helicopter Soc., Inc., September 21 and 22, 1955, pp. 71-90.

3. Heyson, Harry H.: An Evaluation of Linearized Vortex Theory as Applied to Single and Multiple Rotors Hovering In and Out of Ground Effect. NASA TN D-43, 1959.

4. DeFrance, Smith J.: The N.A.C.A. Full-Scale Wind Tunnel. NACA Rep. 459, 1933.

5. Gessow, Alfred, and Myers, Garry C., Jr.: Aerodynamics of the Helicopter. The Macmillan Co., c.1952.

6. Bailey, F. J., Jr.: A Simplified Theoretical Method of Determining the Characteristics of a Lifting Rotor in Forward Flight. NACA Rep. 716, 1941.

7. Jacobs, Eastman N., and Sherman, Albert: Airfoil Section Characteristics as Affected by Variations of the Reynolds Number. NACA Rep. 586, 1937.

8. Jewel, Joseph W., Jr., and Harrington, Robert D.: Effect of Compressibility on the Hovering Performance of Two 10-Foot-Diameter Helicopter Rotors Tested in the Langley Full-Scale Tunnel. NACA RM L58B19, 1958.

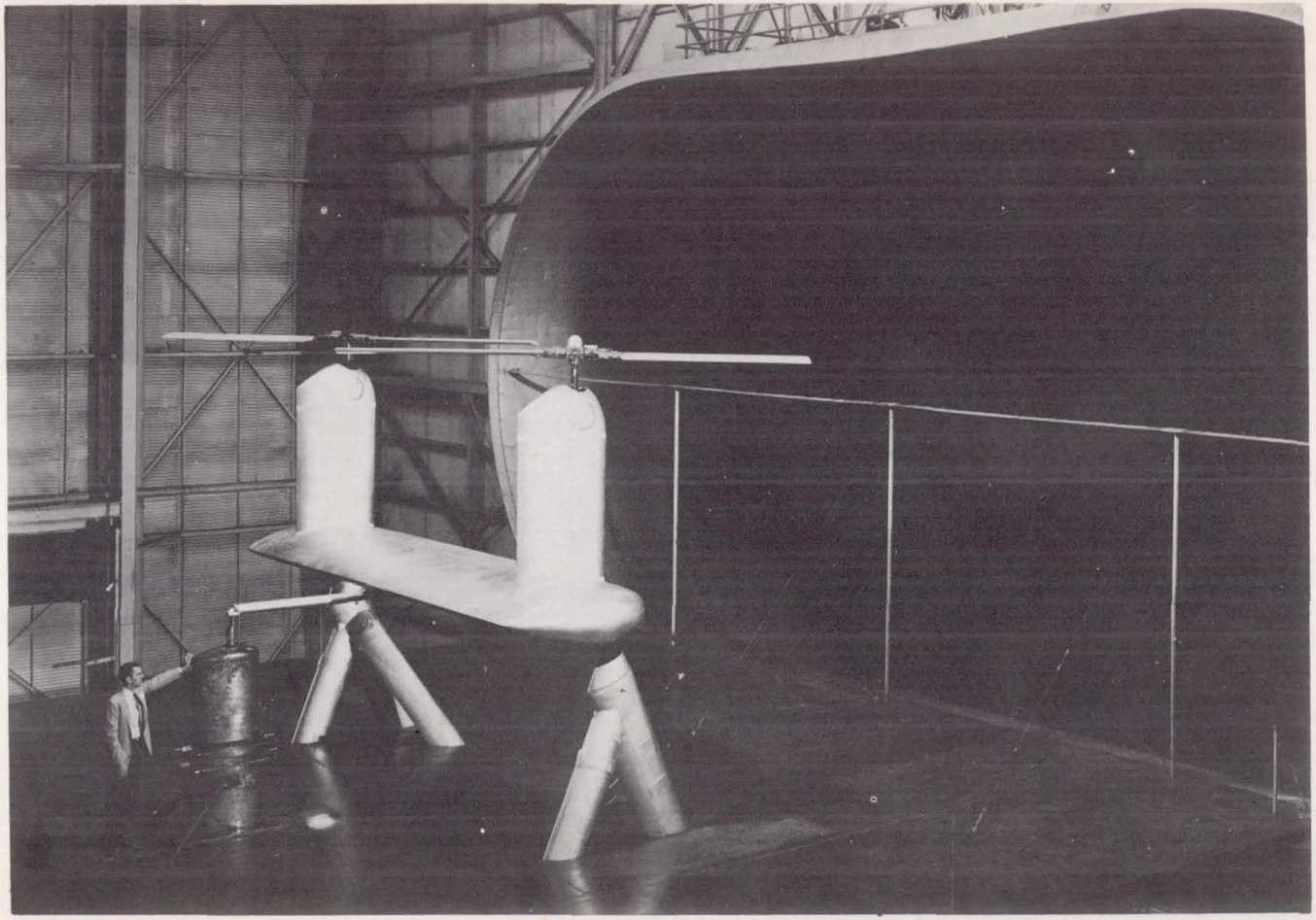

(a) General arrangement of side-by-side rotor system in the Langley full-scale tunnel. L-96045

Figure 1.- Equipment used in side-by-side hovering-performance test.

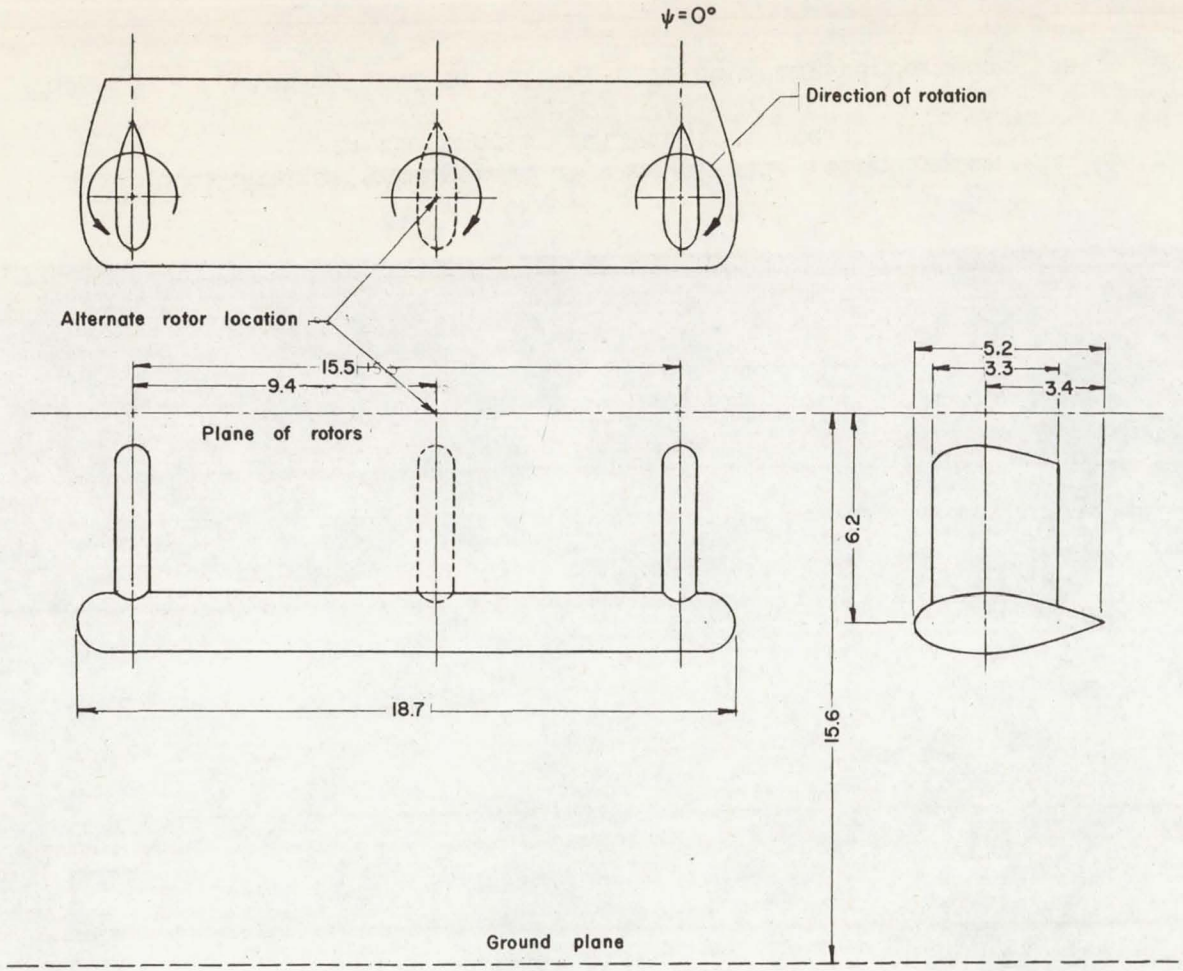

(b) Three-view drawing of side-by-side rotor apparatus showing alternate rotor location. All dimensions are in feet.

Figure 1.- Continued.

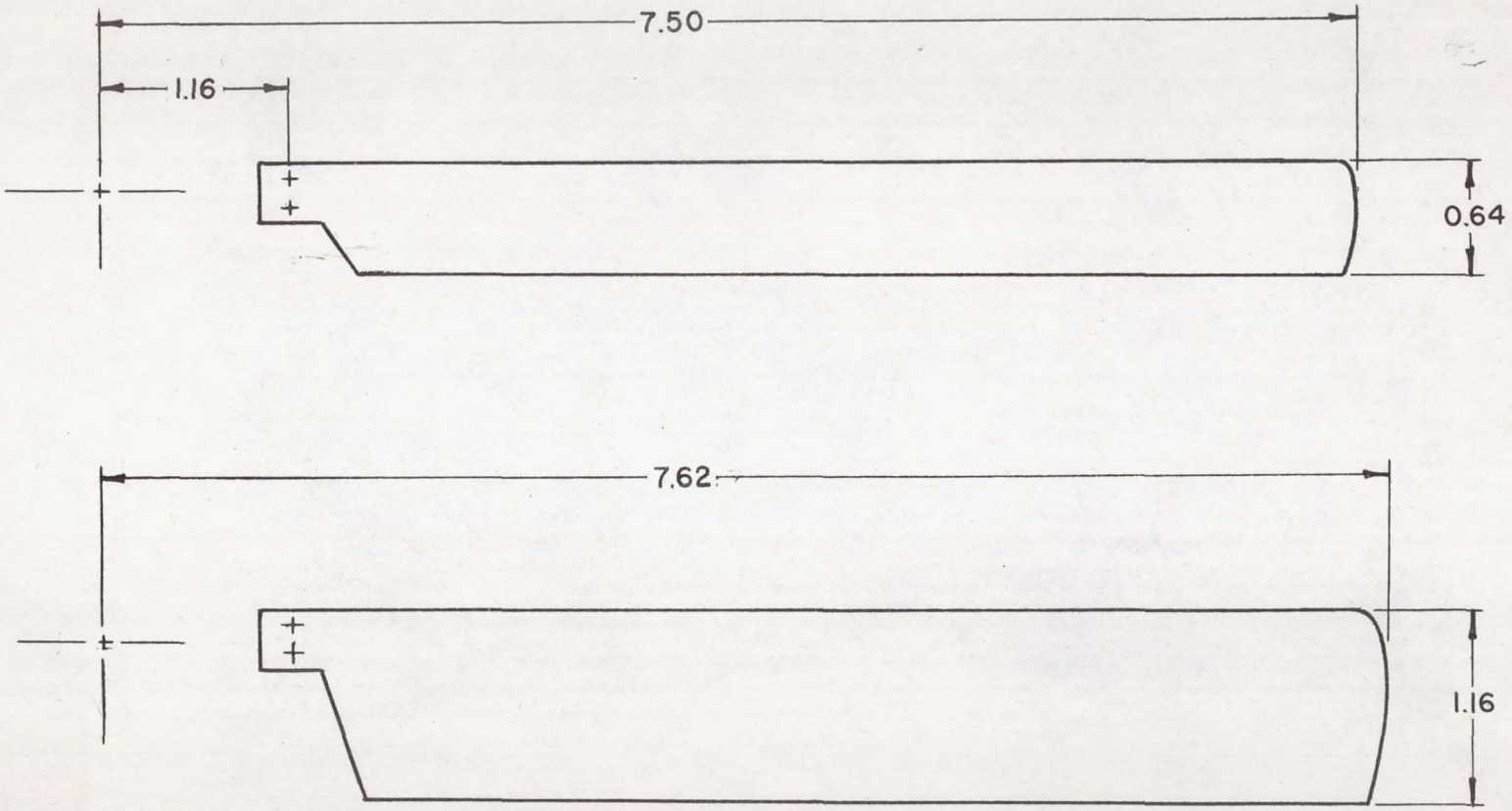

(c) Sketch of blades used in tests. All dimensions are in feet.

Figure 1.- Concluded.

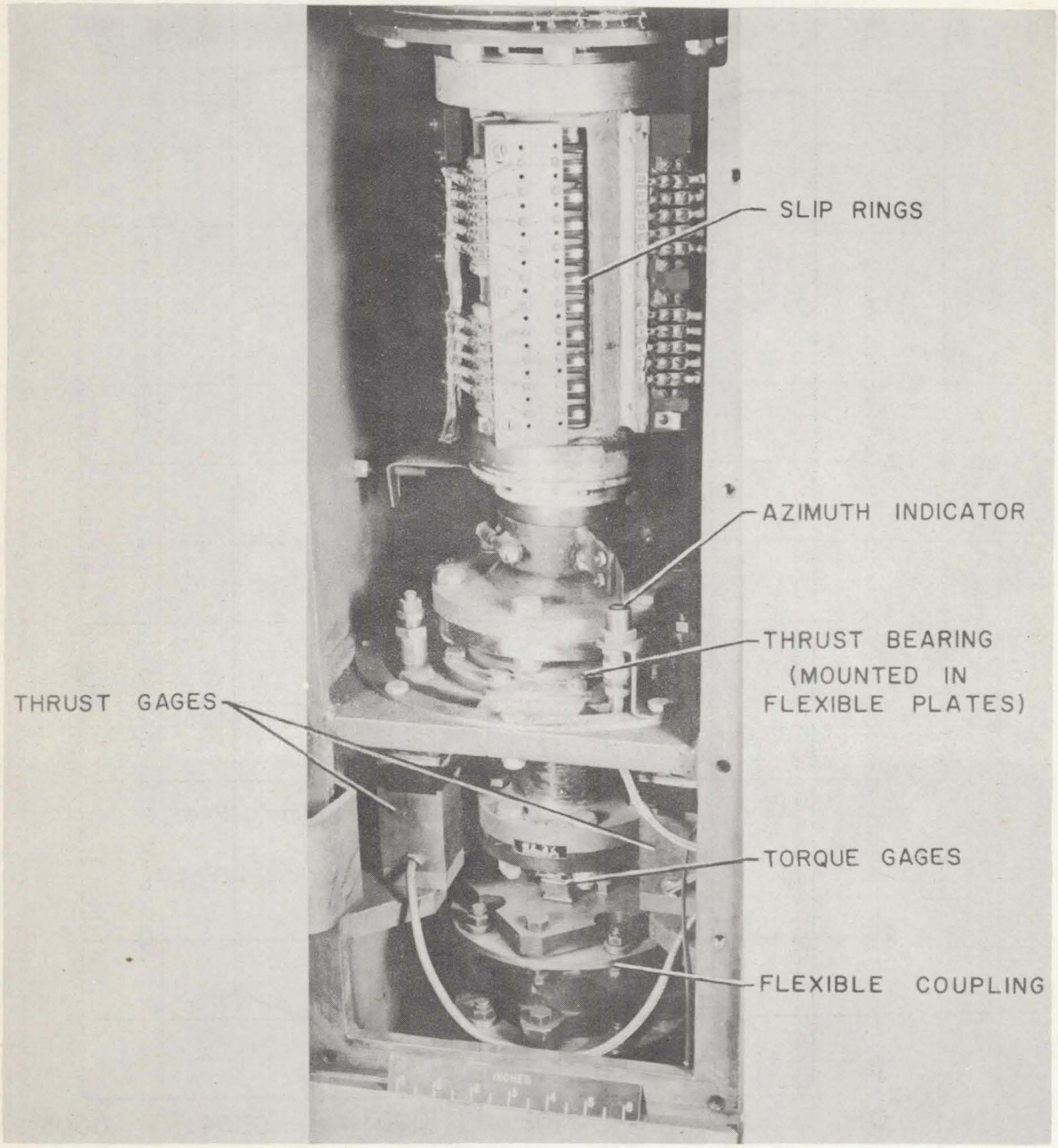

Figure 2.- Force-measuring system. L-58-621a.1

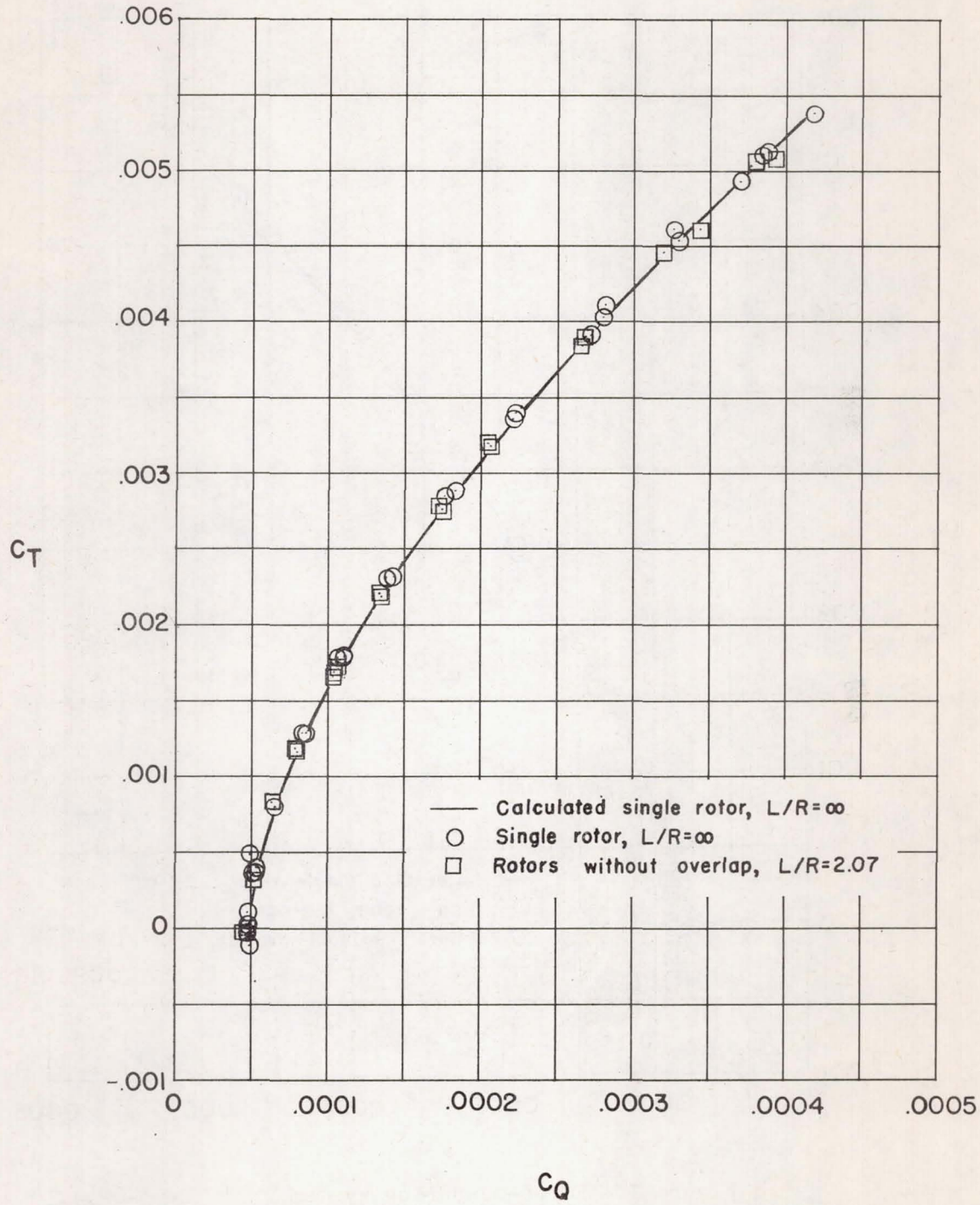

Figure 3.- Comparison of measured hovering performance with single-rotor calculations (σ = 0.0543).

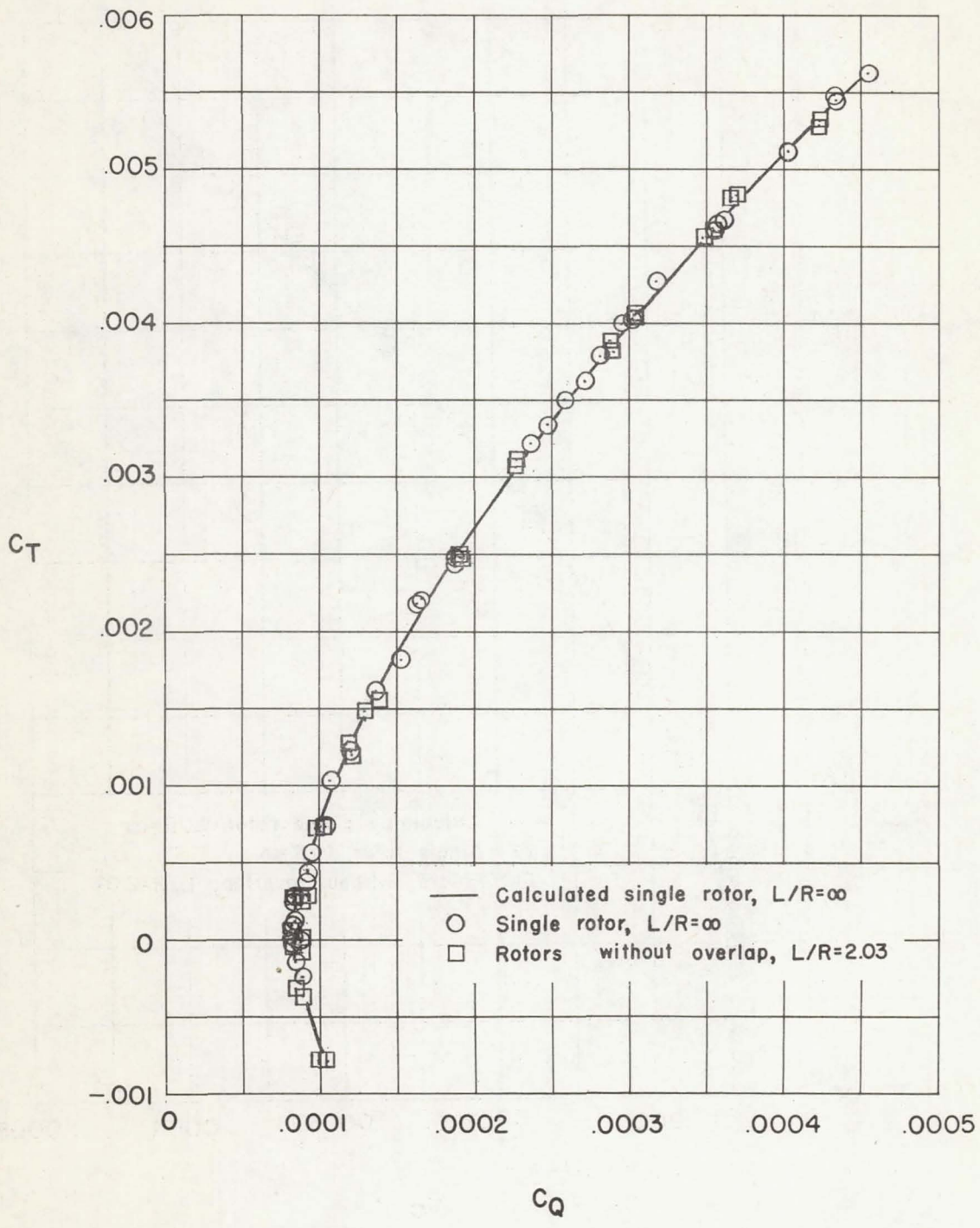

Figure 4.- Comparison of measured hovering performance with single-rotor calculations (σ = 0.0968).

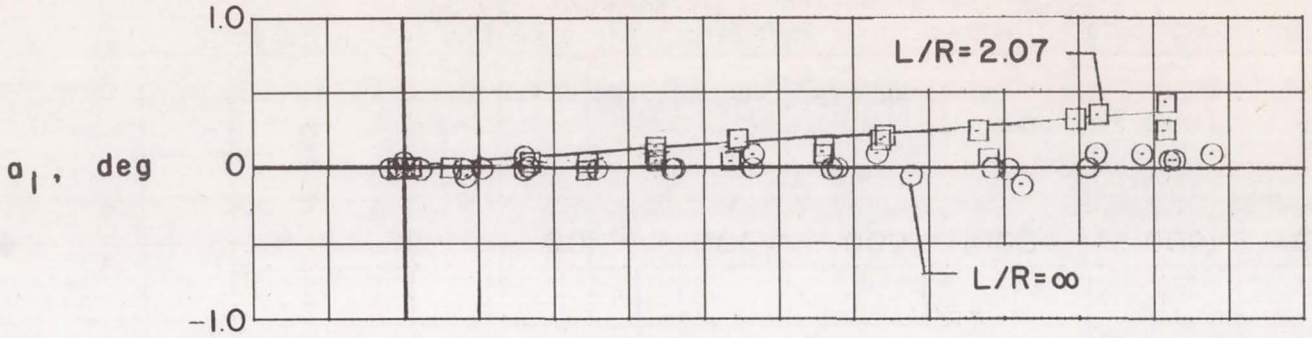

(a) Longitudinal flapping.

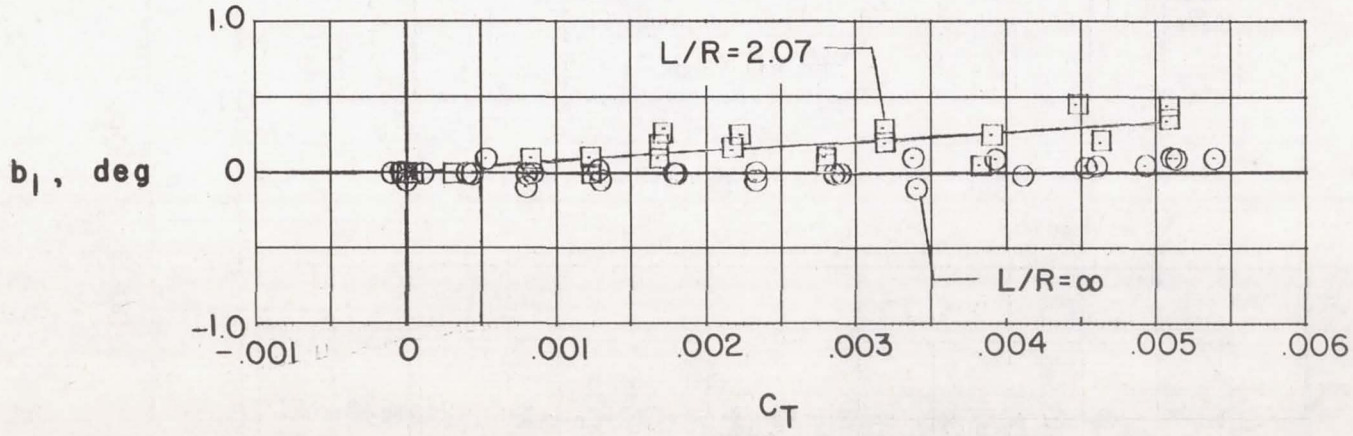

(b) Lateral flapping.

Figure 5.- Measured equivalent flapping coefficients of a single rotor and of rotors without overlap (σ = 0.0543).

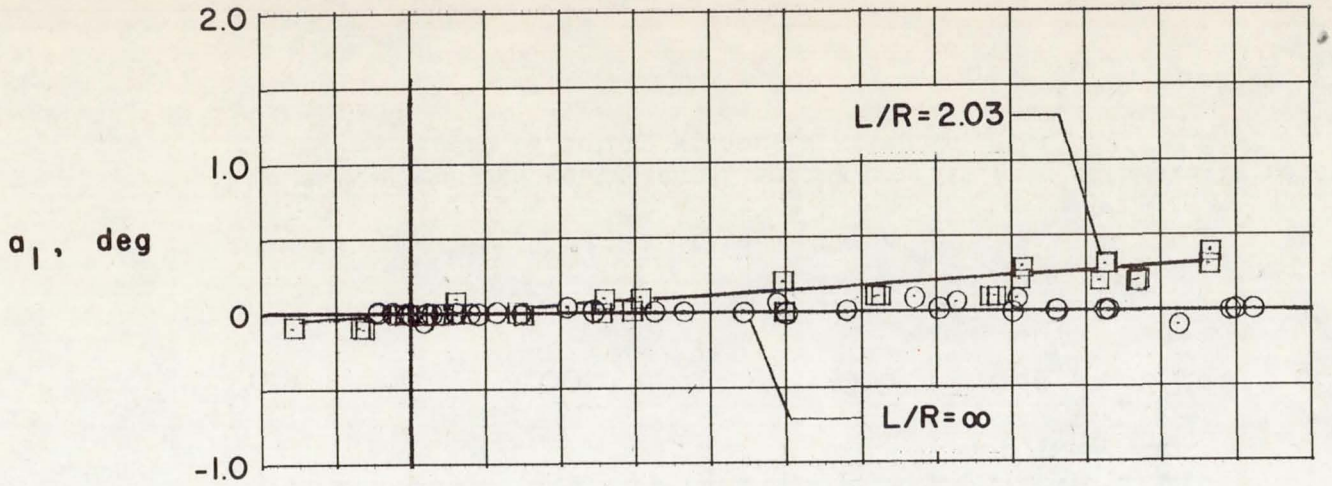

(a) Longitudinal flapping.

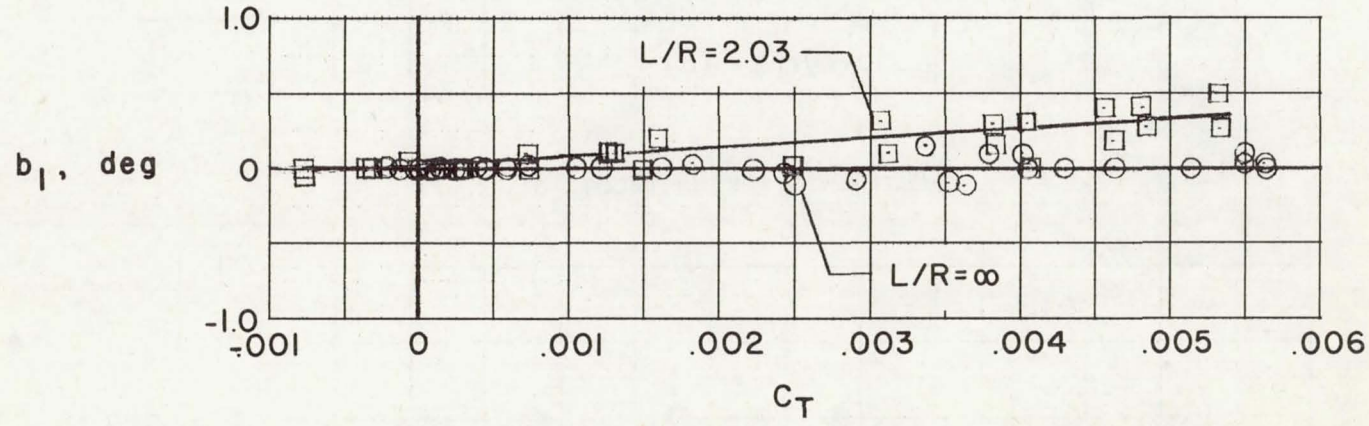

(b) Lateral flapping.

Figure 6.- Measured equivalent flapping coefficients of a single rotor and of rotors without overlap (σ = 0.0968).

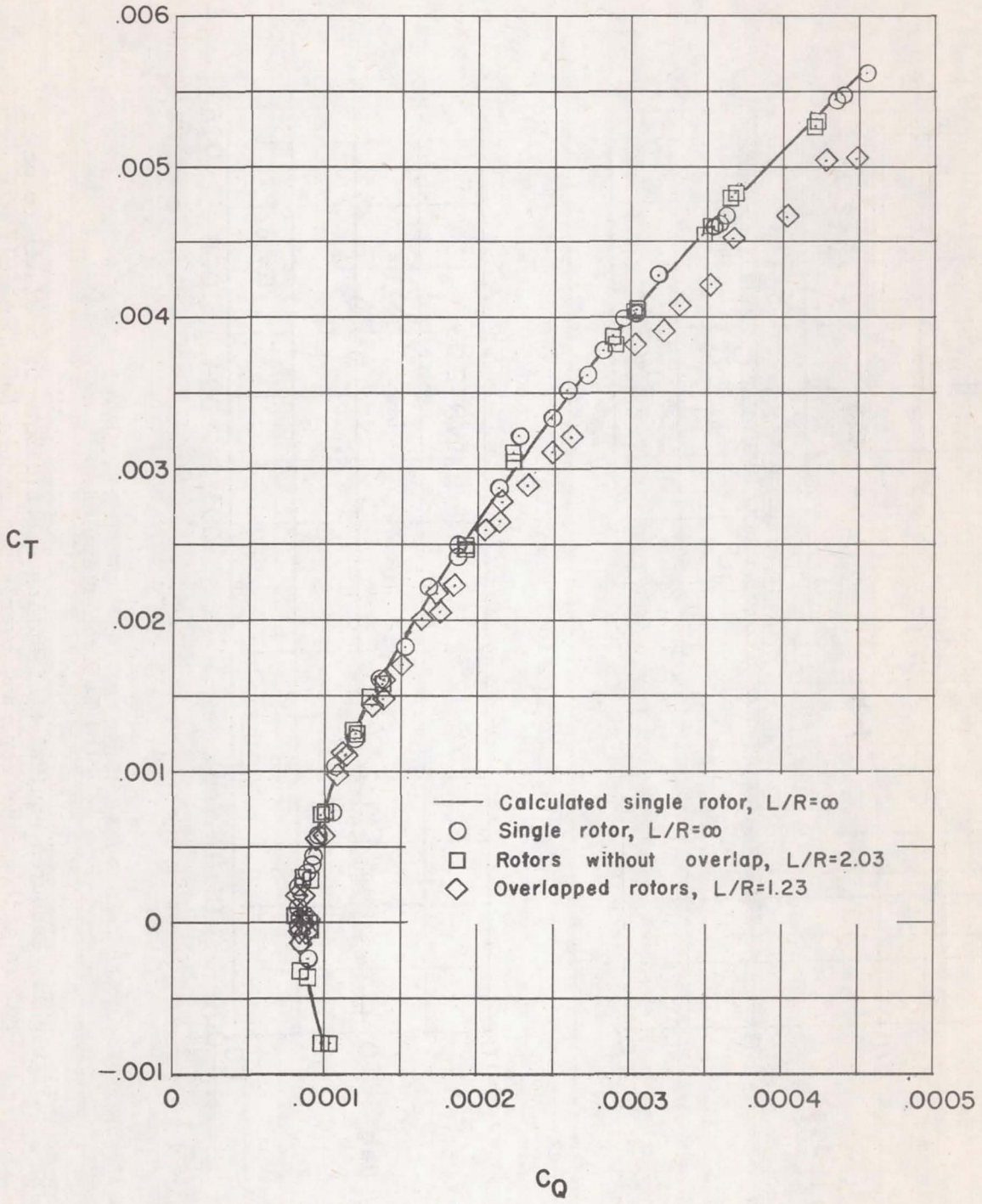

Figure 7.- Comparison of measured hovering performance with single-rotor calculations (σ = 0.0968).

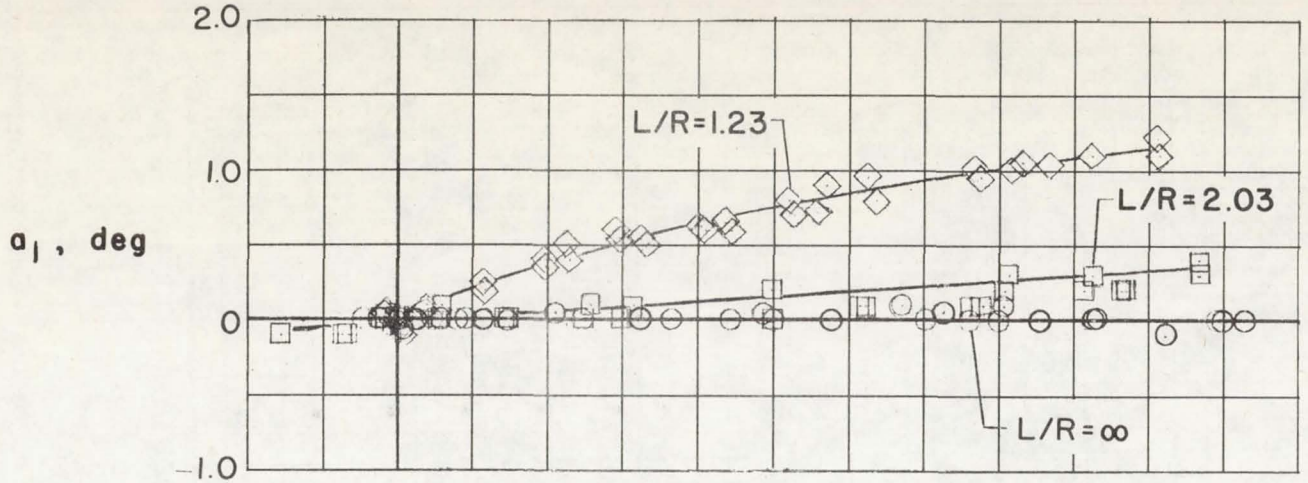

(a) Longitudinal flapping.

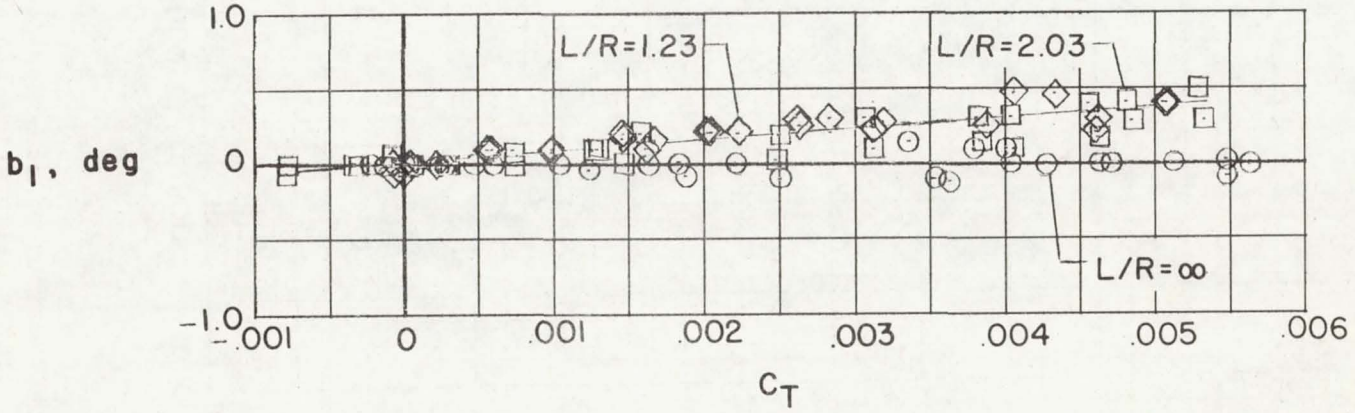

(b) Lateral flapping.

Figure 8.- Measured equivalent flapping coefficients of a single rotor, rotors without overlap, and overlapped rotors (σ = 0.0968).

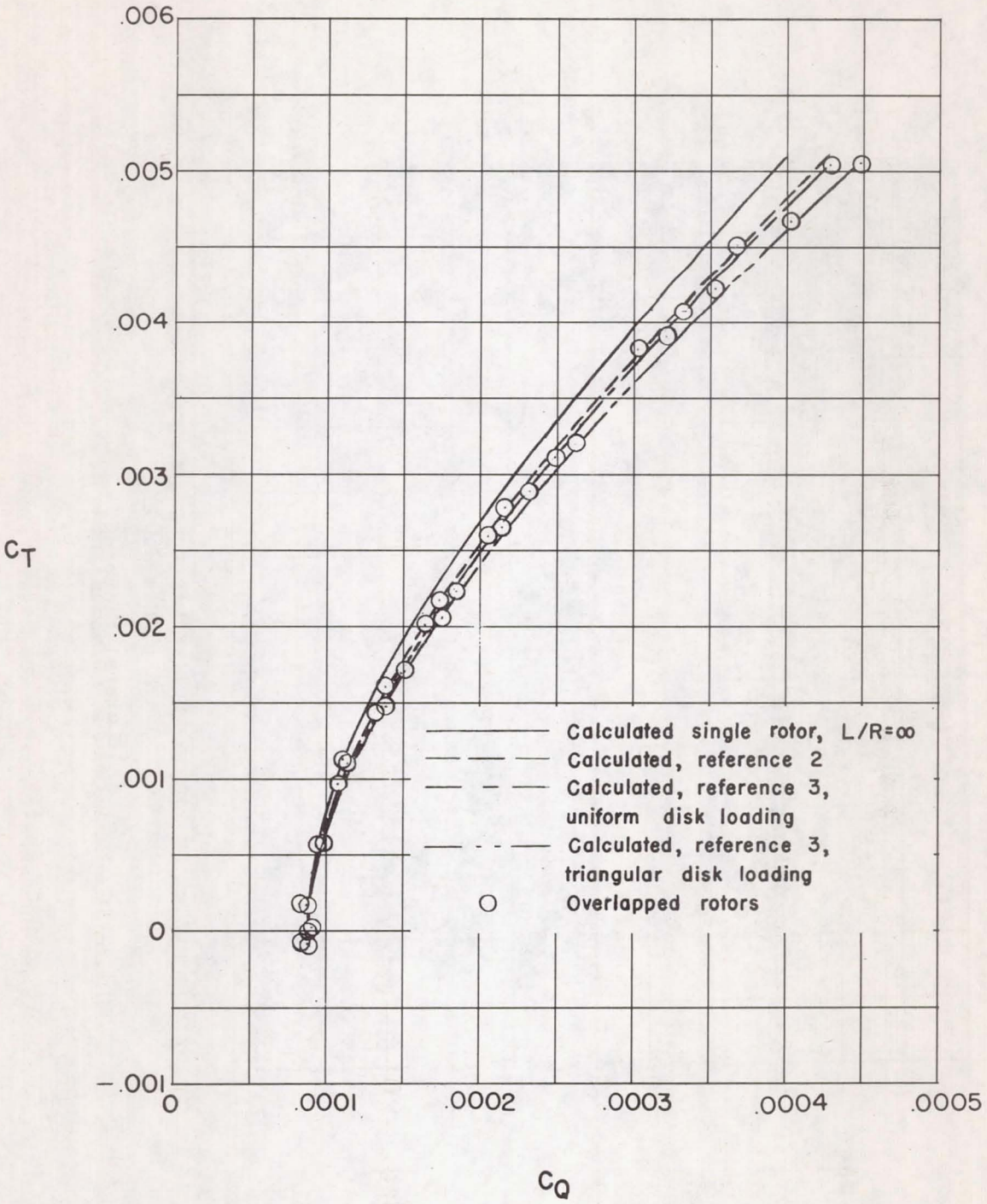

Figure 9.- Comparison of overlapped-rotor measurements with overlapped-rotor calculations (σ = 0.0968; L/R = 1.23).

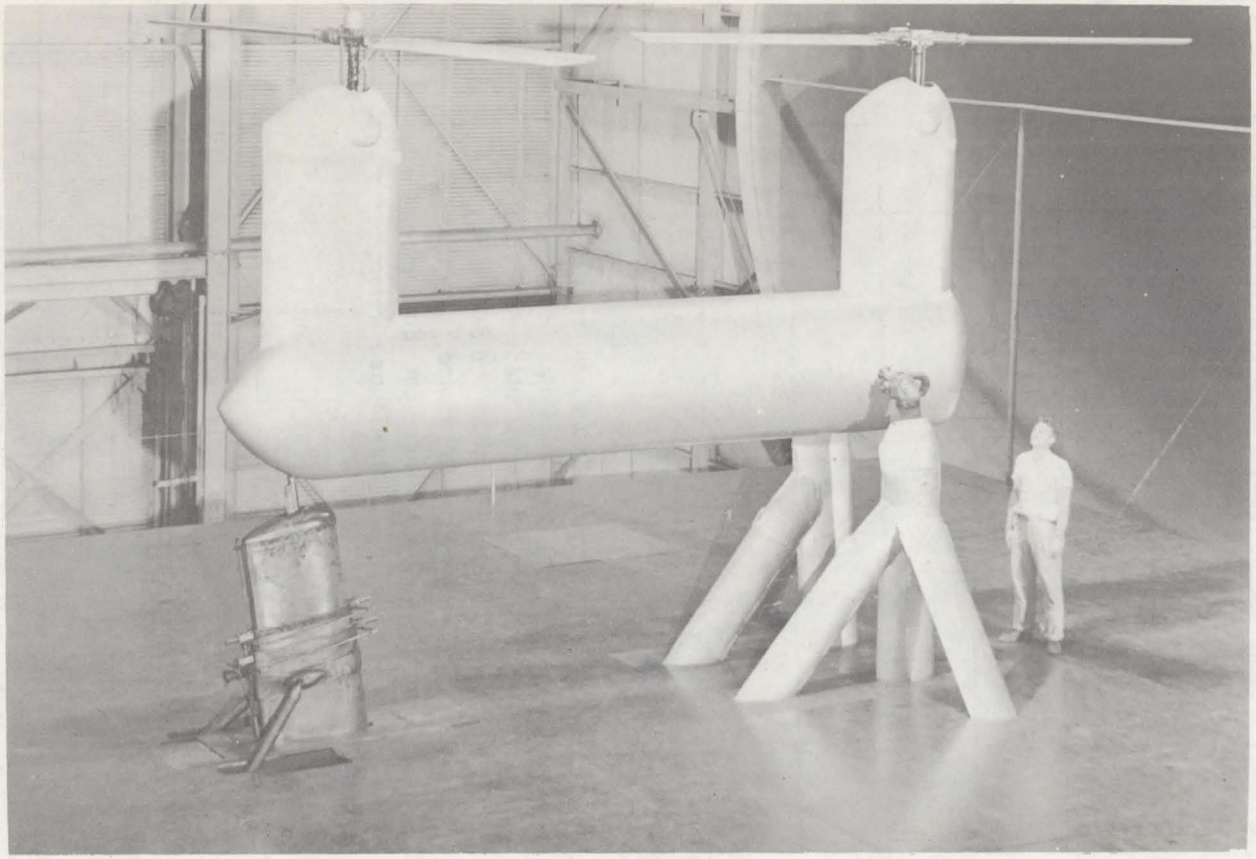

(a) Model mounted in Langley full-scale tunnel to represent a tandem helicopter (L/R = 2.03). L-95193

Figure 10.- Model used in tandem rotor tests.

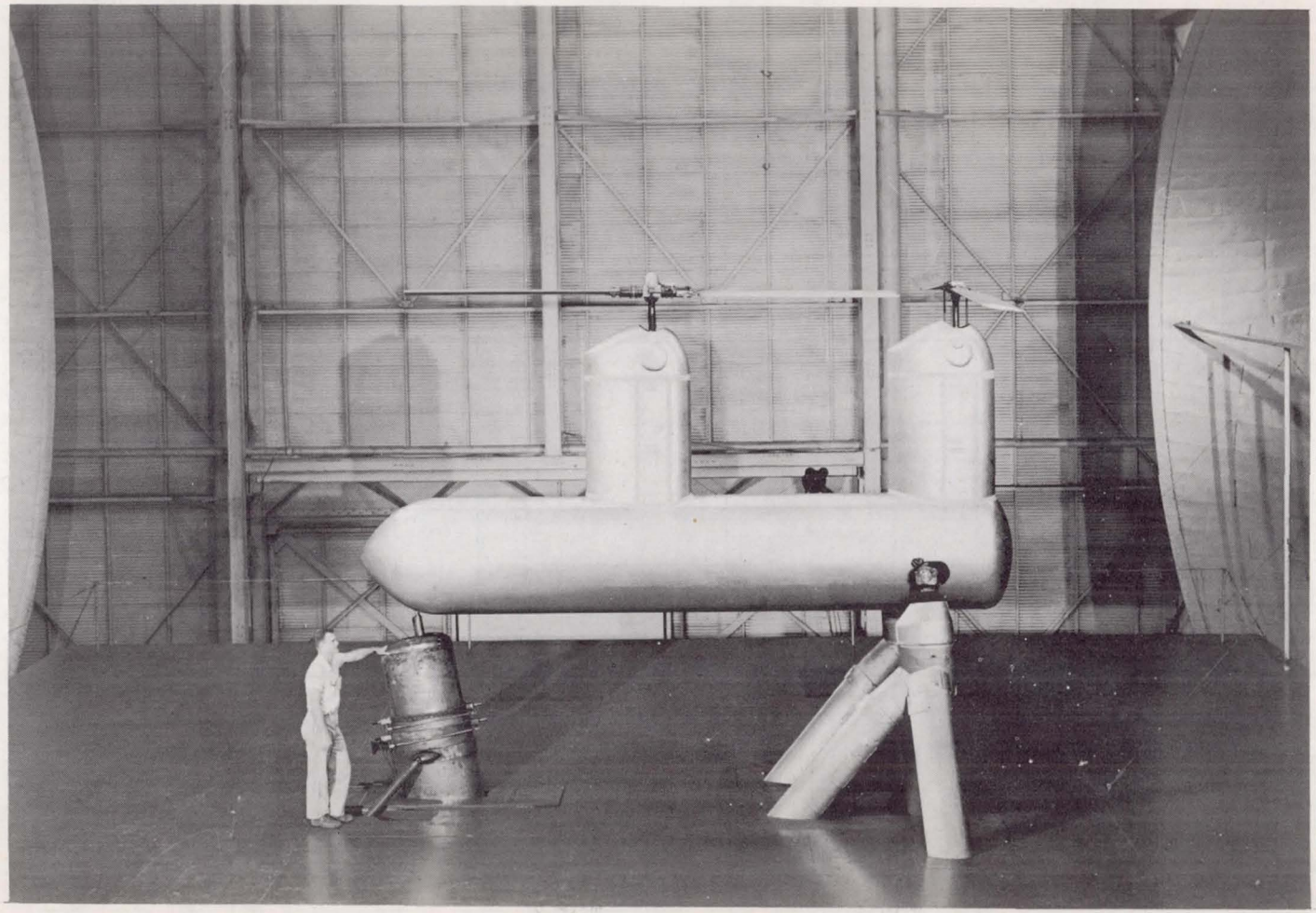

(b) Alternate rotor location for tandem configuration (L/R = 1.23). L-95399

Figure 10.- Concluded.

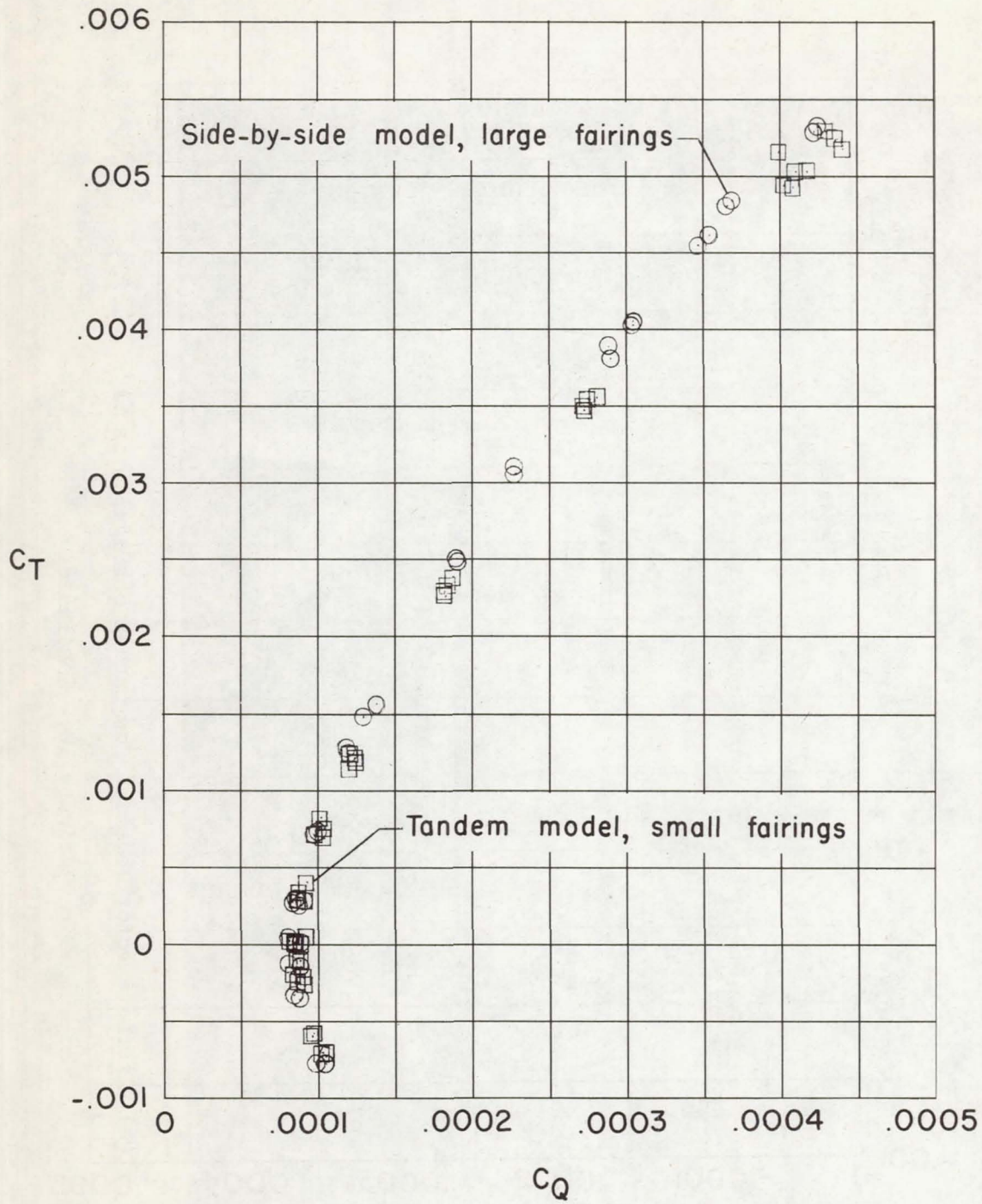

Figure 11.- Comparison of side-by-side and tandem-rotor hovering measurements (σ = 0.0968; L/R = 2.03).

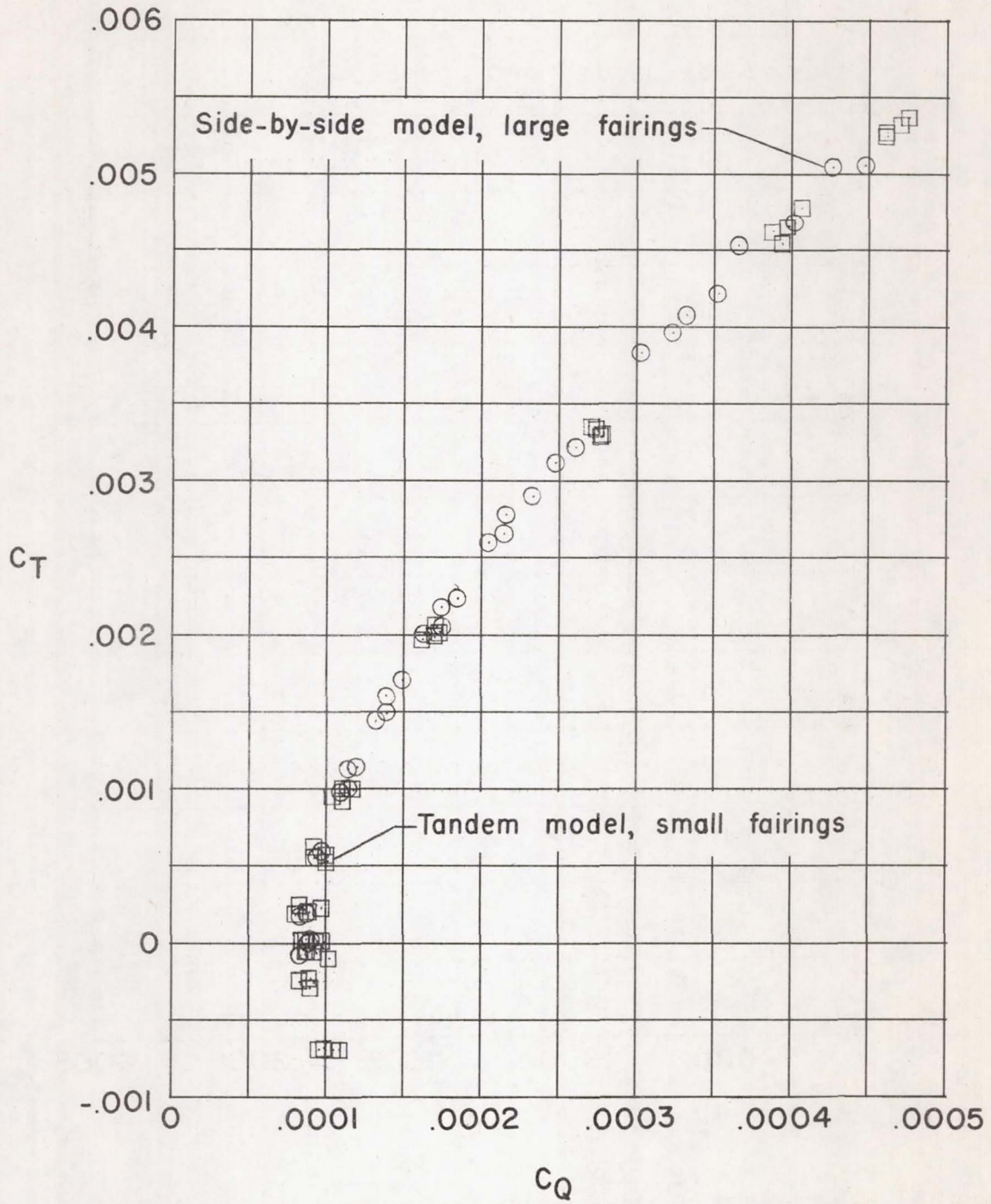

Figure 12.- Comparison of side-by-side and tandem-rotor hovering measurements (σ = 0.0968; L/R = 1.23).